Supplementary Information (SI) for Materials Advances.

SUPPORTING INFORMATION

Enhancing Electrochromic and Electrofluorochromic Performance of Molecular Electrochromes by Their Covalent Immobilization to Nanoparticles

Mohan Raj Anthony Raj,[1] Sacha Porlier,[1] Ram Restikian,[1] W. G. Skene[1,2*]

[1] Département de chimie, Université de Montréal, Montréal, QC, Canada

[2]Institut Courtois, Université de Montréal, Montreal, QC, Canada

Table of Contents

General Details

Materials and methods

ITO coated glass substrates (Delta Technologies) with 2.5 cm x 2.5cm x 0.07 cm dimensions were washed with copious amounts of deionized water. After, they were sonicated in acetone for 15 minutes, followed by sonication with isopropanol (IPA) for another 15 minutes. The cleaned substrates were then dried with a flow of nitrogen. The substrates were next treated with UV plasma for 30 minutes. An ITO nanoparticle suspension (ITO_{np}) was coated on the ITO coated glass substrates by doctor blading followed by drying at 100 °C for 1 hour. The ITO_{np} coated substrate was submerged in an ethanol solution of **1** (100 μM) overnight. The coated substrates were then rinsed with ethanol to remove any physisorbed **1** and dried with a flow of nitrogen.

3D raster profile images of the ITO_{np} coated substrates were obtained with a profilometer (Bruker Dektak). Cyclic voltammetry was done with $LiClO_4$ (0.1 M) in propylene carbonate (PC).

XPS measurement details

X-ray photoelectron spectroscopy (XPS) measurements were performed using a Thermo Scientific Nexsa G2 XPS spectrometer with an Al Kα monochromatic X-ray source (1486.68 eV). A spot size of 400 μm was used for all measurements. The pass energy was set to 200 eV and the step size to 1 eV to acquire survey spectra. High-resolution scans (C_{1s}, O_{1s}, P_{2p}, In_{3d}, In_{3p}, and In MNN) were measured with a pass energy of 50 eV and a step size of 0.1 eV. A dual-beam flood gun is used to prevent sample charging. Binding energy values can be corrected with reference to the adventitious C_{1s} C-C peak at 284.8 eV. The data were processed using Thermo Avantage software, version 6.7.0 and calibrated to adventitious carbon (284.8 eV) using the smart peak background and the Gauss-Lorentz mix convolve peak fitting fixed at 30%. The peaks for each element were fixed the same fwhm. Fitted data were exported and replotted in OriginPro ver. 2025.

Electrochromism

Electronic absorption spectra of the monolayer in dichloromethane were measured using a combined UV-vis NIR absorption spectrometer (Varian-Cary 7000). Spectroelectrochemical measurements were done by placing the monolayer bonded to ITO_{np} (working electrode) in a quartz cuvette with a Teflon separator along with Pt wire as counter electrode, Ag wire as pseudo-reference electrode, and $LiClO_4$ (0.1 M) in propylene carbonate as electrolyte. The potential was applied using potentiostat (Biologic SP300).

Electrofluorochromism

Spectroelectrofluorochromic measurements were carried out with a steady-state spectrometer by exciting with a 450 W Xenon arc lamp (Edinburgh Instruments FLSP-920). The half-cell device was placed at 45° with respect to the excitation light for the emitting light to be detected by the PMT detector. The potential was applied with a potentiostat (Biologic SP300). In one case, the entire emission spectrum was collected contingent on applied potential when exciting at 450nm. In the other case, the emission at 600 nm was continuously recorded contingent on applied potential with potential switching between 1.1 V and -0.2 V at intervals of 1 min and 2 min, respectively.

Synthetic Details

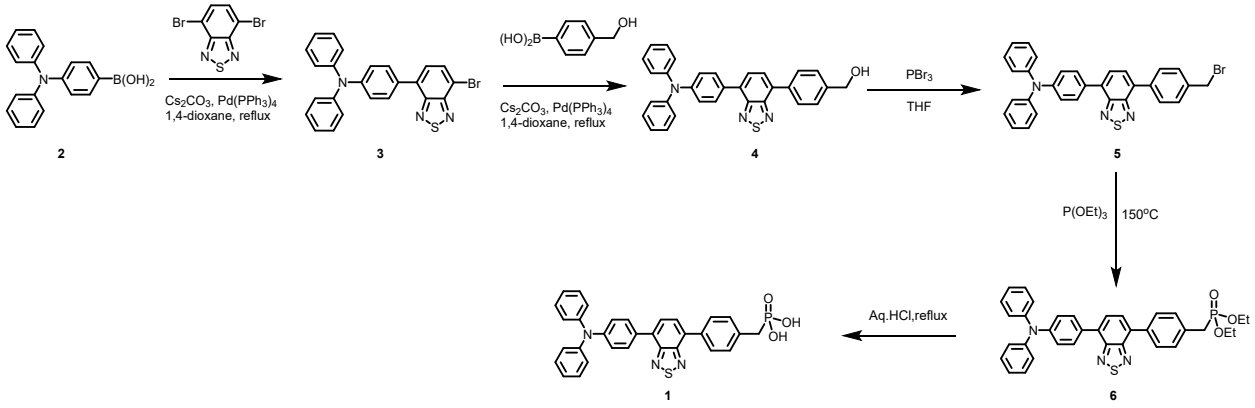

Figure S1. Synthetic scheme for the preparation of the combined electrochrome/electrofluorochrome for its covalent immobilization on ITO nanoparticles.

4-(7-Bromobenzo[c][1,2,5]thiadiazol-4-yl)-*N*,*N*-diphenylaniline (3).[S1] 4,7-Dibromobenzo[c][1,2,5]thiadiazole (2.00 g, 6.8 mmol) and 4-(diphenylamino)- phenyl boronic acid (**2**, 1.97 g, 6.8 mmol) were dissolved in anhydrous and deaerated toluene (50 mL) and an aqueous solution of potassium hydroxide (2 M, 10.2 mL water). A catalytic amount of tetrabutylammonium bromide (TBAB) was then added to the mixture. The reaction mixture was purged with N_2 for 15 mins and a catalytic amount of $Pd(PPh_3)_4$ was added to the mixture under a nitrogen atmosphere. The mixture was heated to 100 ˚C and stirred overnight under nitrogen. After cooling to room temperature, the mixture was washed with water and it was extracted with dichloromethane. The crude product was purified by silica gel column chromatography with dichloromethane/hexane (v/v = 1:6) as the eluent. The title compound was obtained as an orange solid (2.5 g, 68%).^{1}H NMR (400 MHz, $CDCl_3$) δ 7.93 (d, *J* = 7.6 Hz, 1H), 7.84 (d, *J* = 8.8 Hz, 2H), 7.58 (d, *J* = 7.6 Hz, 1H), 7.38 – 7.30 (m, 4H), 7.26 – 7.19 (m, 6H), 7.11 (t, *J* = 7.3 Hz, 2H). ^{13}C NMR ($CDCl_3$, 100 MHz) δ ppm = 154.1, 153.3, 148.6, 147.5, 133.7, 132.5, 130.1, 130, 129.6, 127.5, 125.2, 123.6, 122.7, 112.3. ESI-MS [M+H$^+$]: m/z calcd for $C_{24}H_{16}BrN_3S$ 458.4, found 458.1.

(4-(7-(4-(Diphenylamino)phenyl)benzo[c][1,2,5]thiadiazol-4-yl)phenyl)methanol (4).[S2] 4-(Hydroxymethyl)-phenyl boronic acid (0.497 g, 3.27 mmol), **3** (1.00 g, 2.18 mmol) and cesium carbonate (1.42 g, 4.36 mmol) were dissolved in anhydrous and deaerated 1,4-dioxane (50 mL) and deionized water (10 mL). The reaction mixture was purged with N_2 for 15 mins and a catalytic amount of $Pd(PPh_3)_4$ was added to the mixture under a nitrogen atmosphere. The mixture was heated to 100 ˚C and stirred overnight under nitrogen. After cooling to room temperature, the mixture was washed with water and it was extracted with dichloromethane. The crude product was purified by silica gel column chromatography with dichloromethane/hexane (v/v = 5:1) as eluent. The title compound was obtained as a red solid (0.9 g, 85%).^{1}H NMR (400 MHz, $CDCl_3$) δ 8.01 (d, *J* = 8.4 Hz, 2H), 7.90 (d, *J* = 8.8 Hz, 2H), 7.58 (d, *J* = 8.4 Hz, 2H), 7.36 – 7.30 (m, 4H), 7.26 – 7.19 (m, 6H), 7.07 (t, *J* = 7.3 Hz, 2H) δ 4.83 (d, *J*=6 Hz, 2H; CH2), δ 1.69 (t = 6 Hz, 1H; OH). ^{13}C NMR ($CDCl_3$, 100 MHz) δ ppm = 154.2, 154.1, 148.1, 147.5, 140.9, 136.9, 133.0, 132.3, 130.8, 130.0, 129.9, 129.4, 128.2, 127.3, 127.2, 125.0, 123.4, 122.9, 65.2. ESI-MS [M+H$^+$]: m/z calcd for $C_{31}H_{23}N_3OS$ 486.1626 found 486.1635.

4-(7-(4-(Bromomethyl)phenyl)benzo[c][1,2,5]thiadiazol-4-yl)-*N*,*N*-diphenylaniline (5).[S2] Phosphorus tribromide (156 µL, 0.83 mmol) was added dropwise at 0 °C under a nitrogen atmosphere to a solution of **4** (800 mg, 1.65 mmol) in anhydrous THF (40 mL). After the mixture was stirred at room temperature for 3 h, the reaction mixture was poured into ice water and extracted with toluene (50 mL x 3). The combined organic layers were dried over anhydrous magnesium sulfate and evaporated in vacuo to dry ness. The residue was purified by silica gel column chromatography eluting with chloroform/hexane 1:1 and recrystallized from chloroform/hexane to give red needles (620 mg, 69%). ^{1}H NMR (400 MHz, $CDCl_3$): d=4.62 (s, 2H; CH_2), 7.08 (t, *J*=7.6 Hz, 2H; ArH), 7.2–7.26 (t, *J* = 7.6 Hz 6H; ArH), 7.3-7.35 (t, *J* = 7.6 Hz, 4H; ArH), 7.58 (d, *J*=8.4 Hz, 2H; ArH), 7.78 (dd, *J*=6 Hz, 2H; ArH), 7.92 (d, *J*=8.4 Hz, 2H; ArH),

7.98 ppm (d, *J*=8.4 Hz, 2H; ArH). ^{13}C NMR (100 MHz, $CDCl_3$) δ ppm = 154.2, 154.1, 148.2, 147.4, 137.7, 137.6, 133.2, 131.8, 130.7, 129.9, 129.6, 129.4, 129.4, 128.4, 127.2, 125.0, 123.4, 122.8, 33.3, ESI-MS [M+H$^+$]: m/z calcd for $C_{31}H_{22}BrN_3S$ 547.0791 found 547.0820.

Diethyl (4-(7-(4-(diphenylamino)phenyl)benzo[c][1,2,5]thiadiazol-4-yl)benzyl)phosphonate (6). Triethyl phosphite (625 µL, 3.64 mmol) and **5** (200 mg, 0.364 mmol) were heated at 150 °C for 12 h. The reaction mixture was then poured into hexane (150 mL) after cooling. The precipitates were collected by filtration and washed thoroughly with hexane to give **6** (115 mg, 83%) as an orange solid. ^{1}H NMR (400 MHz, $CDCl_3$): δ=1.3 ppm (t, 6H; CH_3), δ=3.25 ppm (d, *J*=21.6Hz, 2H; PCH_2), δ= 4.12 ppm (m, 4H; OCH_2), 7.08 (t, *J*=7.2 Hz, 2H; ArH), 7.21–7.26 (t, d = 8.0 Hz, 6H; ArH), 7.31-7.35 (t, *J* = 7.2Hz, 4H; ArH), 7.49 (dd, *J*=2.4, 10.8 Hz, 2H; ArH), 7.791 (d, *J*=7.9 Hz, 1H; ArH), 7.798 (d, *J*=7.9 Hz, 1H; ArH), 7.90 (d, *J*=8.4 Hz, 2H; ArH), 7.96 ppm (d, *J*=7.6 Hz, 2H, ArH); ^{13}C NMR ($CDCl_3$, 100 MHz) δ ppm =154.2, 154.1, 148.1, 147.5, 136.1, 136.0, 132.8, 132.2, 131.8, 131.76, 130.9, 130.1, 130.0, 129.9, 129.4, 129.3, 128.1, 127.3, 124.94, 123.3, 122.8, 62.2, 62.1, 34.3, 32.5, 16.43, 16.42. ^{31}P NMR (108.1 MHz, δ ppm = 21.69). ESI-MS [M+H$^+$]: m/z calcd for $C_{35}H_{32}N_3O_3PS$ 606.1971 found 606.1975.

(4-(7-(4-(Diphenylamino)phenyl)benzo[c][1,2,5]thiadiazol-4-yl)benzyl)phosphonic acid (1). **6** (150 mg) was added to a round-bottom flask followed by conc. HCl (10 mL) and deionized water (5 mL) and then refluxed for 24 hours. The reaction mixture was neutralized with sodium bicarbonate and extracted with dichloromethane (3 x 50 mL). The title compound was only sparingly soluble in dichloromethane. The solvent was removed under reduced pressure and the compound dried (100 mg, 73.5%). ^{1}H NMR (400 MHz, CD_3OD): δ= 3.14 ppm (s, 1H; PCH_a), δ=3.19 ppm (s, 1H; PCH_b), δ= 7.08 (t, *J*=7.2 Hz, 2H; ArH), 7.14–7.16 (m, 6H; ArH), 7.31-7.35 (t, *J* = 7.6 Hz, 4H; ArH), 7.49 (dd, *J*=2.0, 10.4 Hz, 2H; ArH), 7.84-7.86 (m, 2H; ArH), 7.94-7.98 (m, 4H; ArH); ^{13}C NMR ($CDCl_3$, 100 MHz) δ ppm =154.1, 153.9, 148.0, 147.6, 134.7, 132.6, 132.1, 131.2, 129.8, 129.7, 129.6, 129.1, 128.6, 128.5, 127.7, 127.2, 124.5, 124.2, 123.1, 122.5, 53.4. ^{31}P NMR (108.1 MHz, δ ppm = 19.36). ESI-MS [M+NH_4^+]: m/z calcd for $C_{31}H_{24}N_3O_3PS$ 567.1614 found 567.1611.

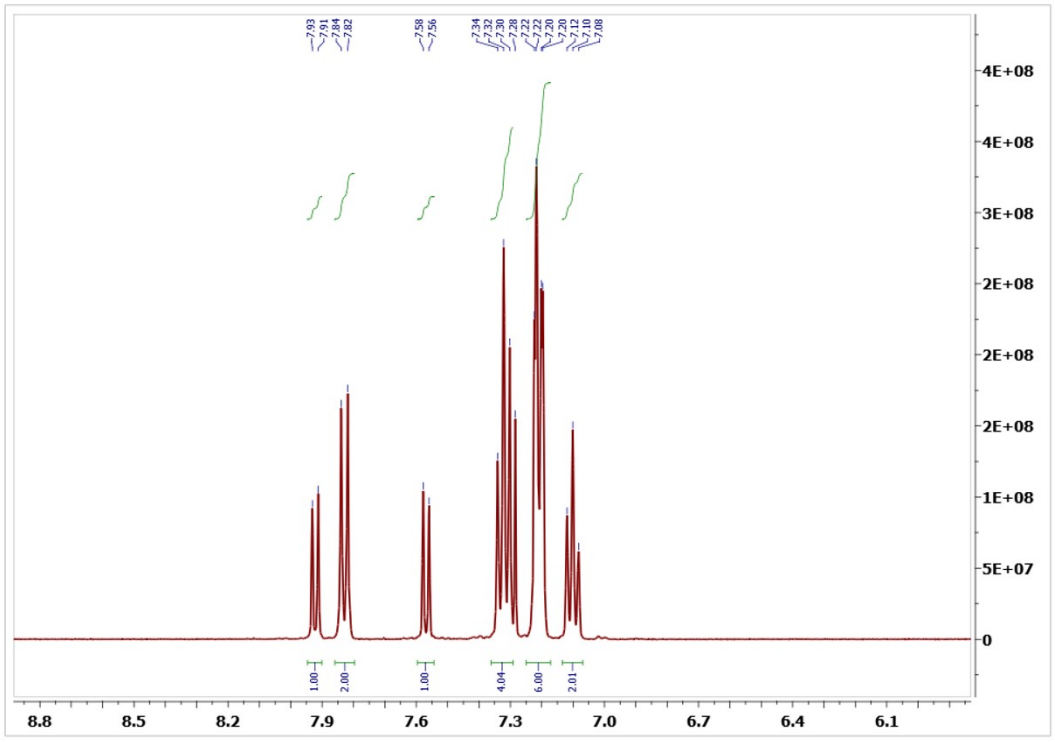

Figure S2. ^{1}H-NMR spectrum of **3** in $CDCl_3$ (400 MHz).

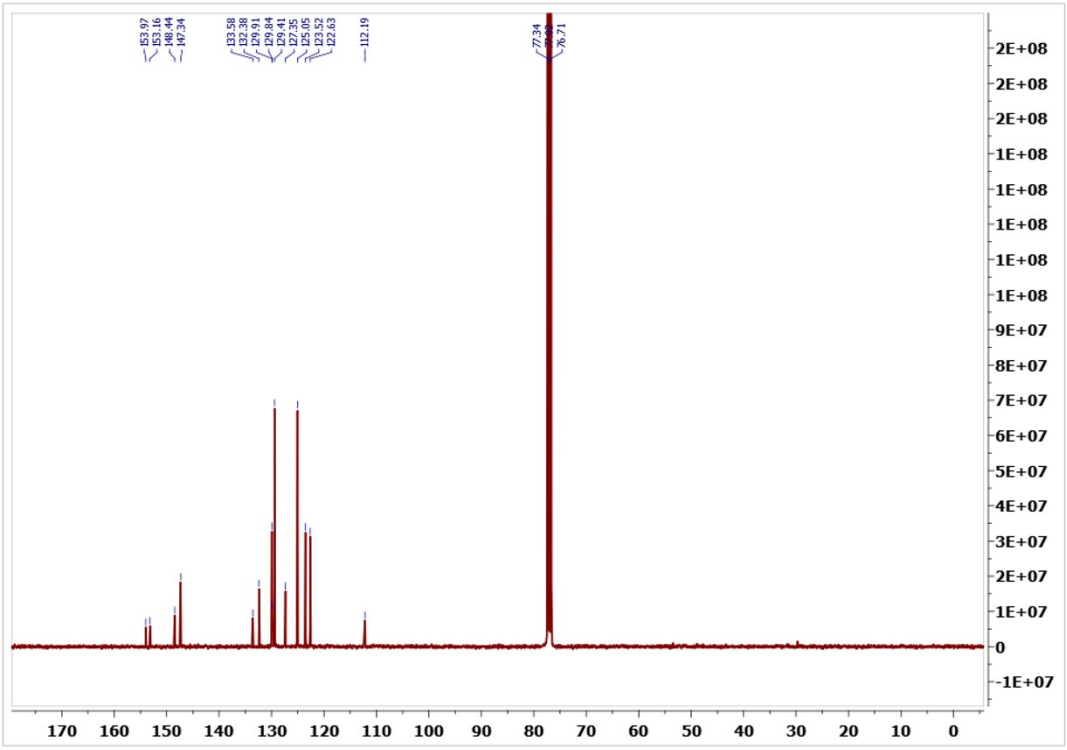

Figure S3. ^{13}C-NMR spectrum of **3** in $CDCl_3$ (100 MHz).

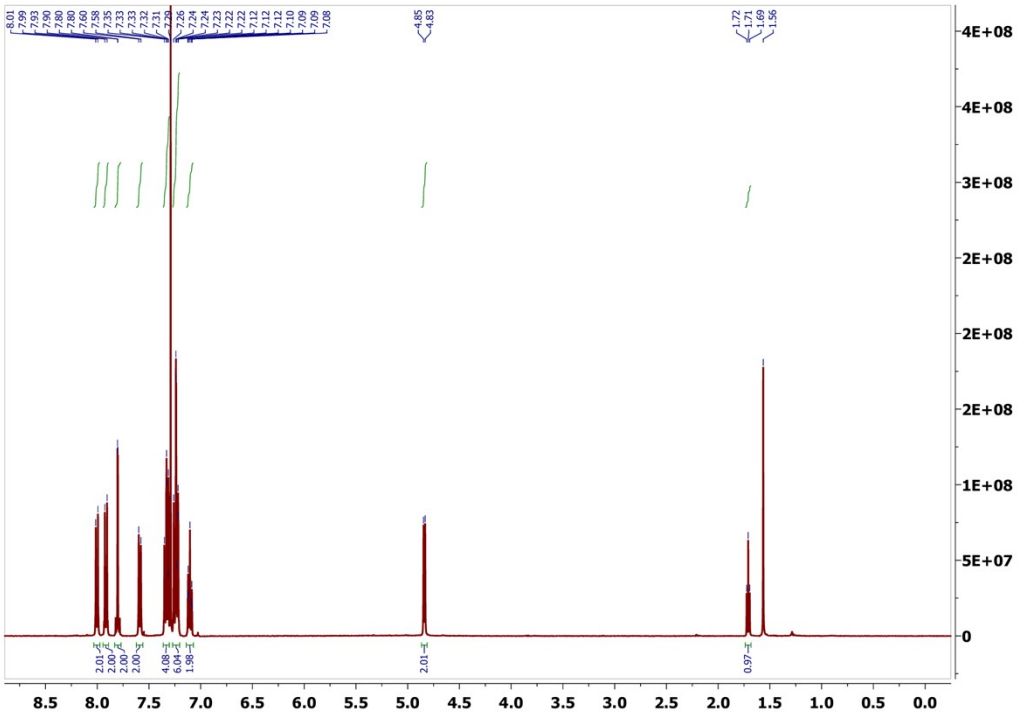

Figure S4. ^{1}H-NMR spectrum of **4** in $CDCl_3$ (400 MHz).

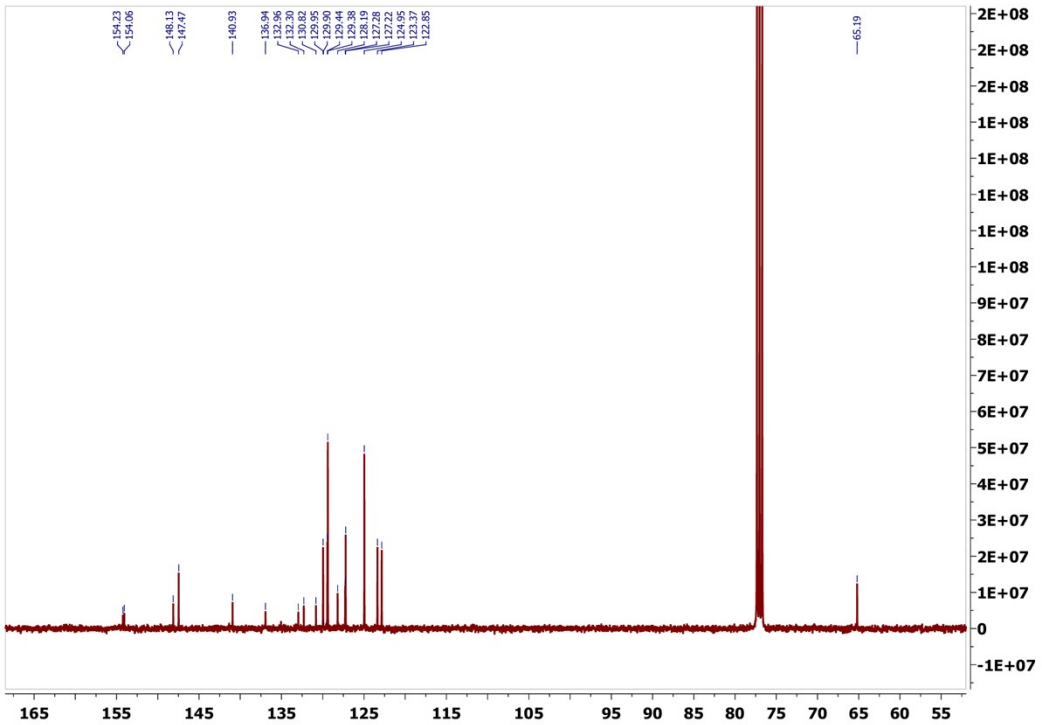

Figure S5. ^{13}C-NMR spectrum of **4** in $CDCl_3$ (100 MHz).

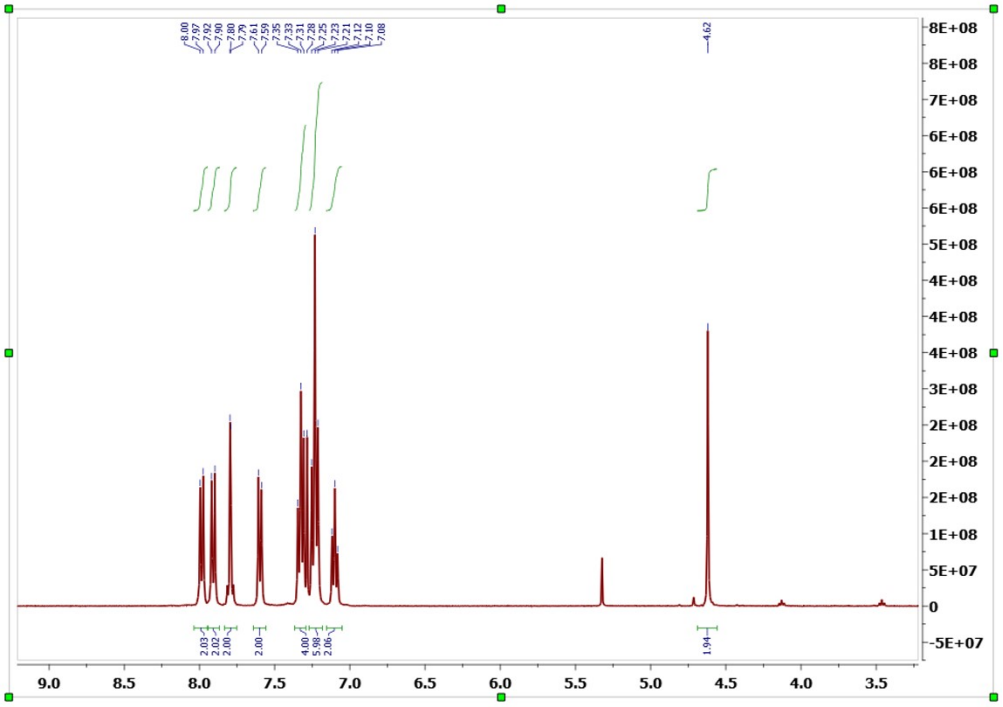

Figure S6. ^{1}H-NMR spectrum of **5** in $CDCl_3$ (400 MHz).

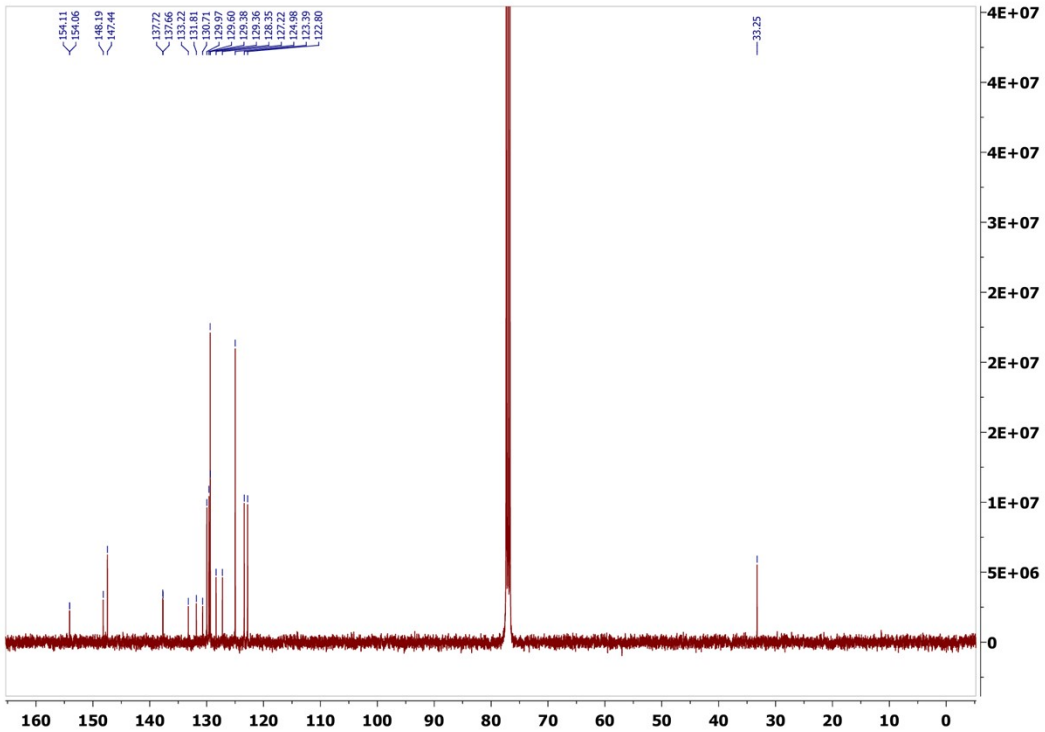

Figure S7. ^{13}C-NMR spectrum of **5** in $CDCl_3$ (100 MHz).

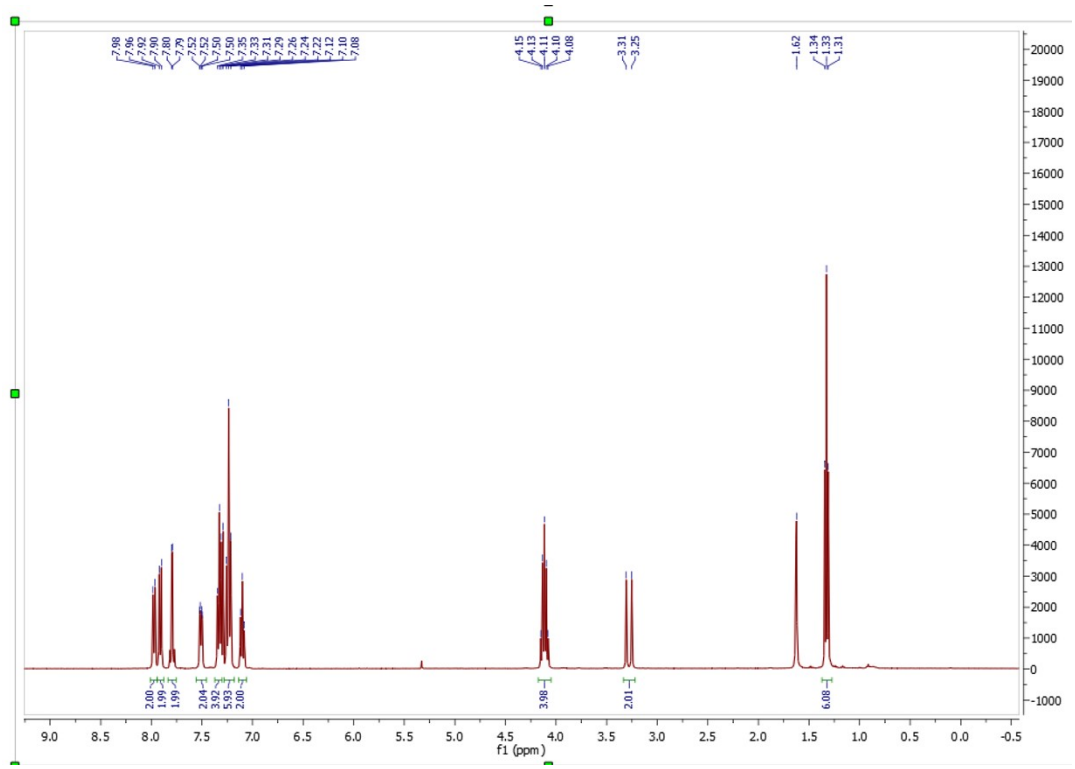

Figure S8. ^{1}H-NMR spectrum of **6** in $CDCl_3$ (400 MHz).

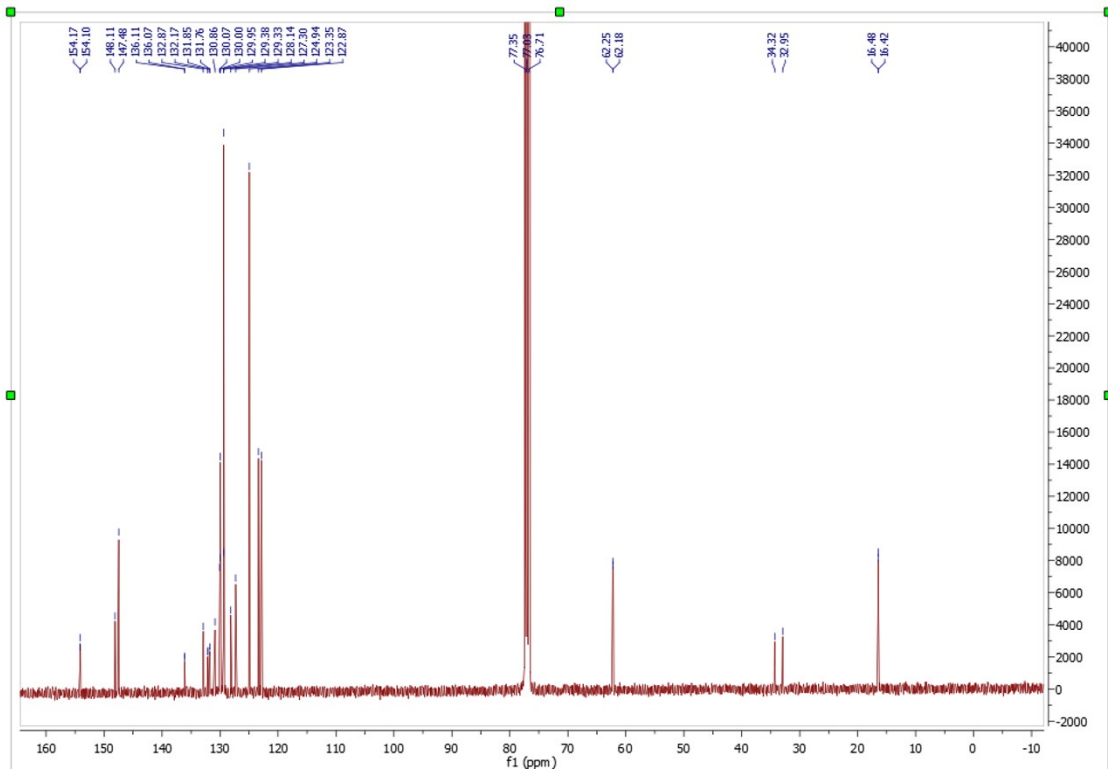

Figure S9. ^{13}C-NMR spectrum of **6** in $CDCl_3$ (100 MHz).

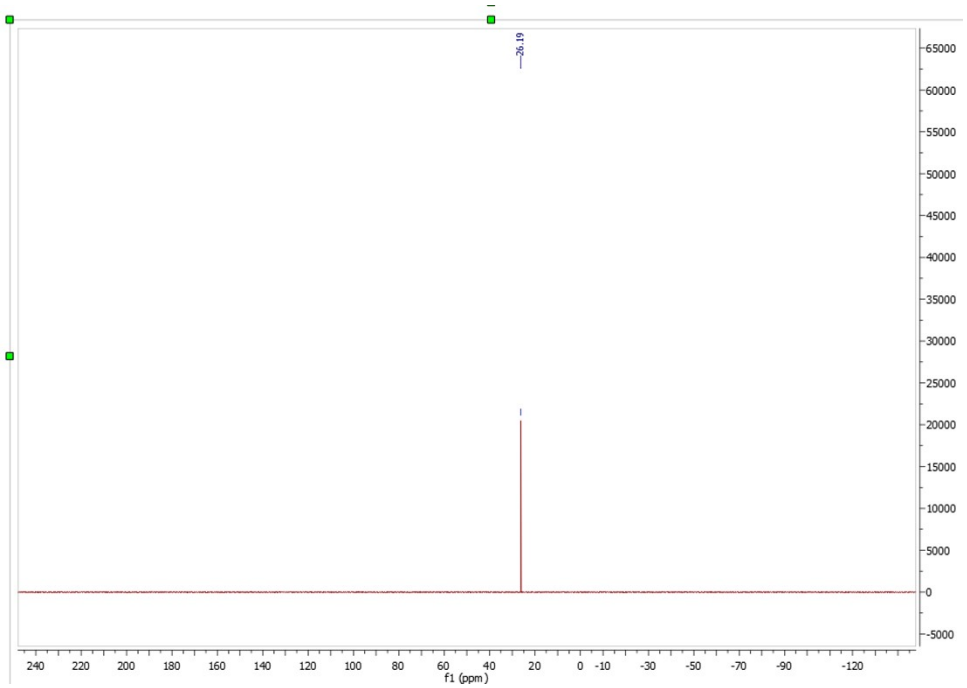

Figure S10. ^{31}P-NMR spectrum of **6** in $CDCl_3$ (100 MHz).

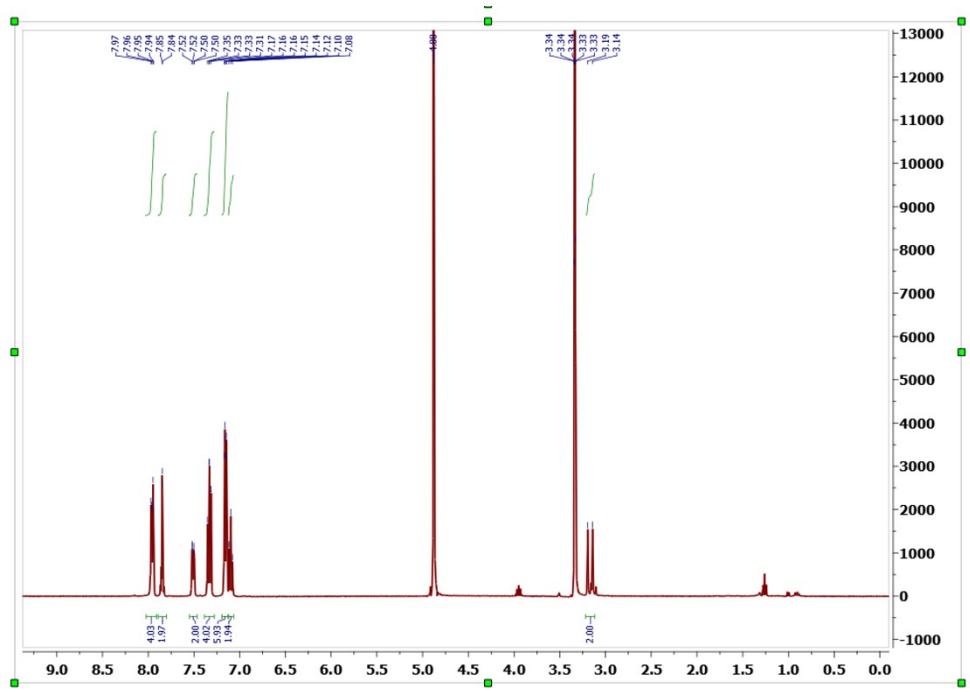

Figure S11. ^{1}H-NMR spectrum of **1** in CD_3OD (400 MHz).

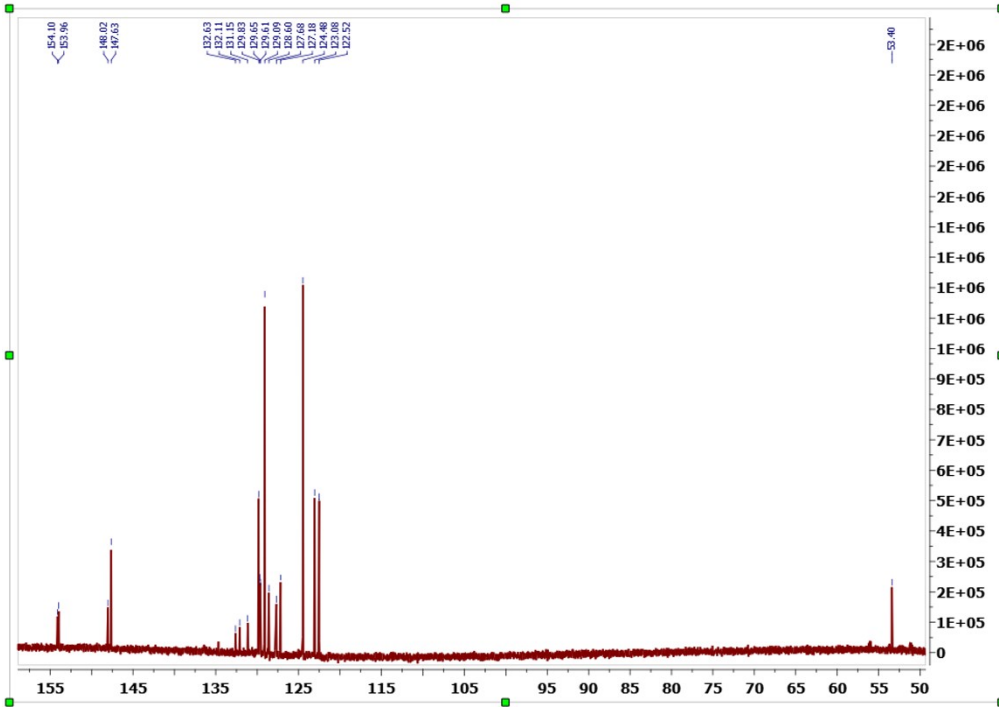

Figure S12. ^{1}H-NMR spectrum of **1** in CD_3OD (100 MHz).

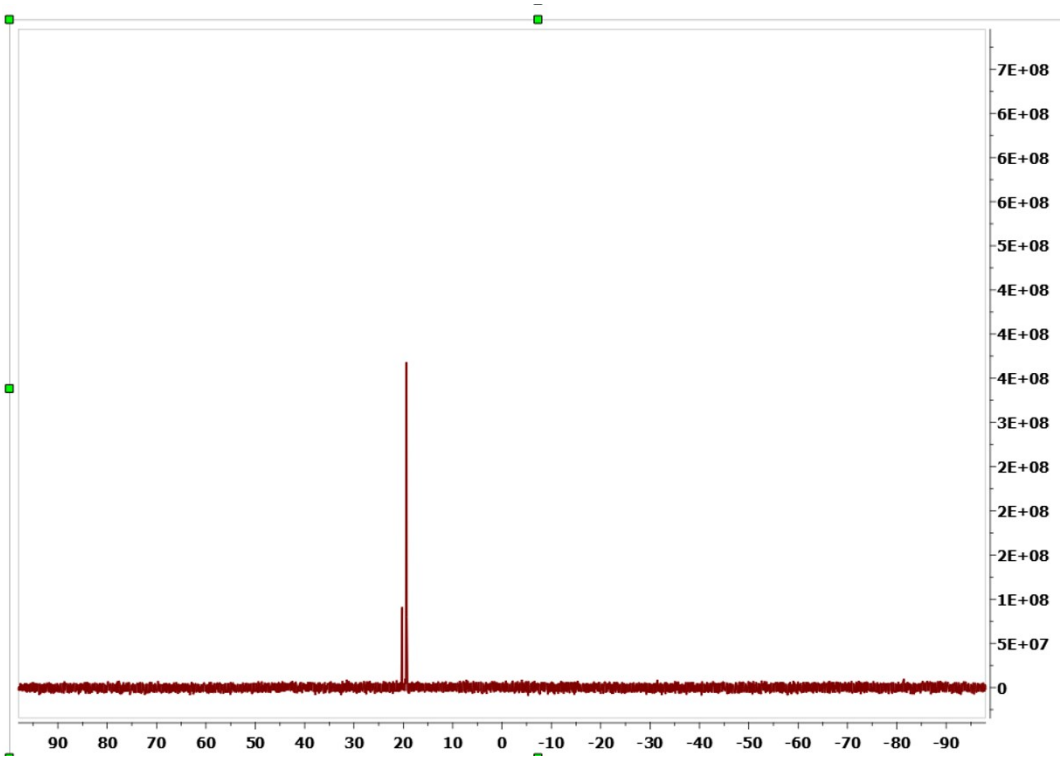

Figure S13. ^{31}P-NMR spectrum of **1** in CD_3OD (108 MHz).

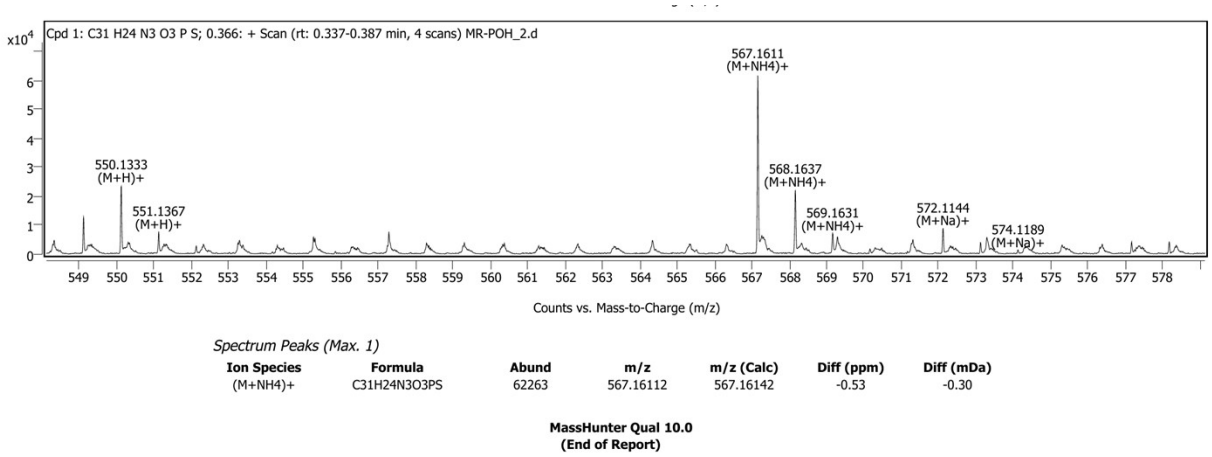

Figure S14. High-resolution mass spectrometry data of **1**.

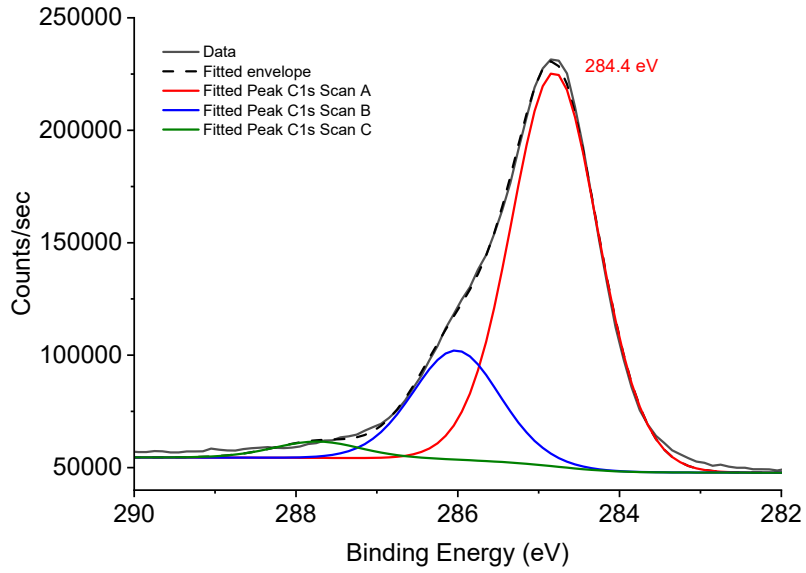

Figure S15. XPS C_{1s} spectrum of **1** bound to ITO_{np} with peaks calibrated.

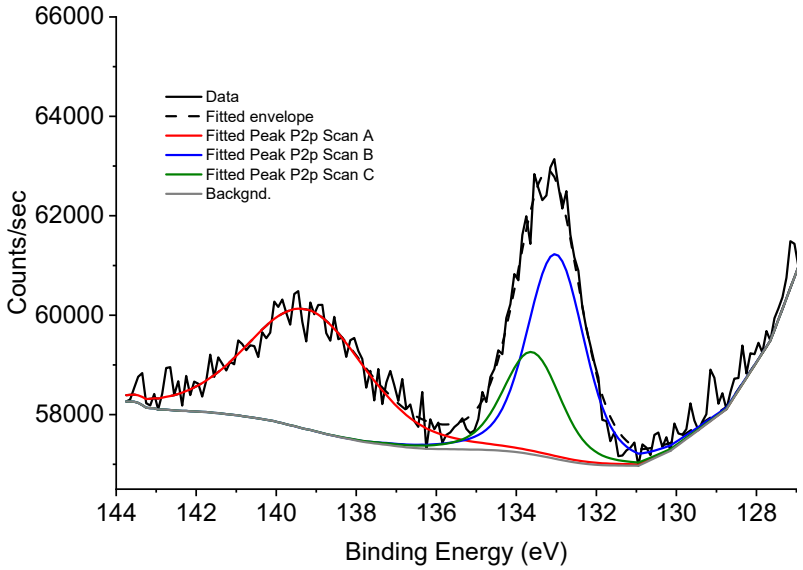

Figure S16. XPS P_{2p} spectrum of **1** bound to ITO_{np} with peaks calibrated to adventitious carbon and fitted for spin orbit coupling in 1:2 ratio.

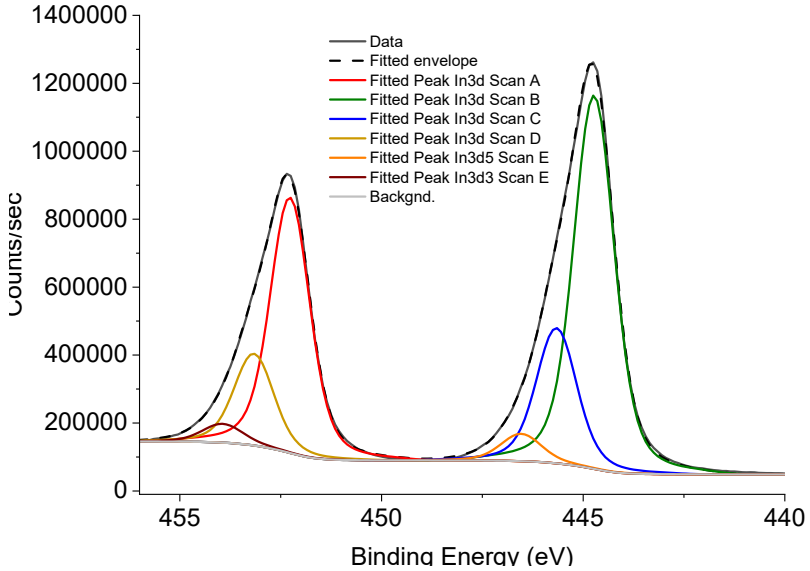

Figure S17. XPS In_{3d} spectrum of **1** bound to ITO_{np} with peaks calibrated to adventitious carbon.

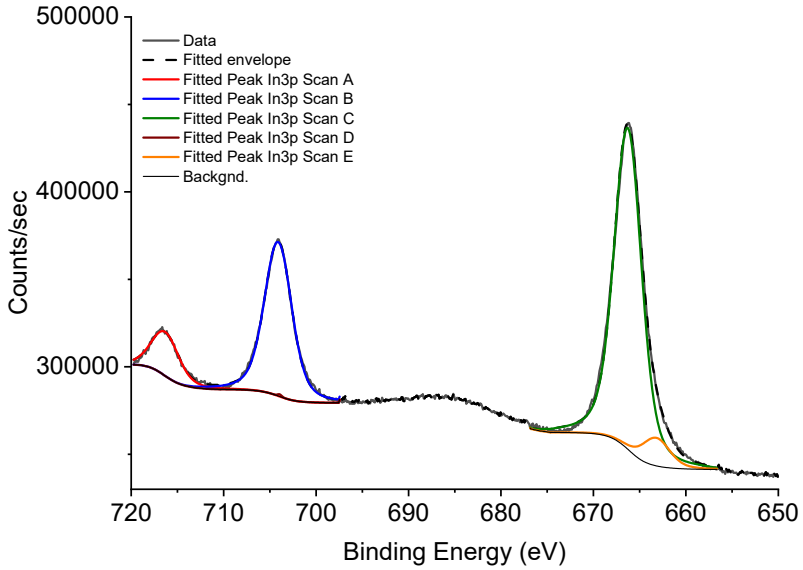

Figure S18. XPS In_{3p} spectrum of **1** bound to ITO_{np} with peaks calibrated to adventitious carbon.

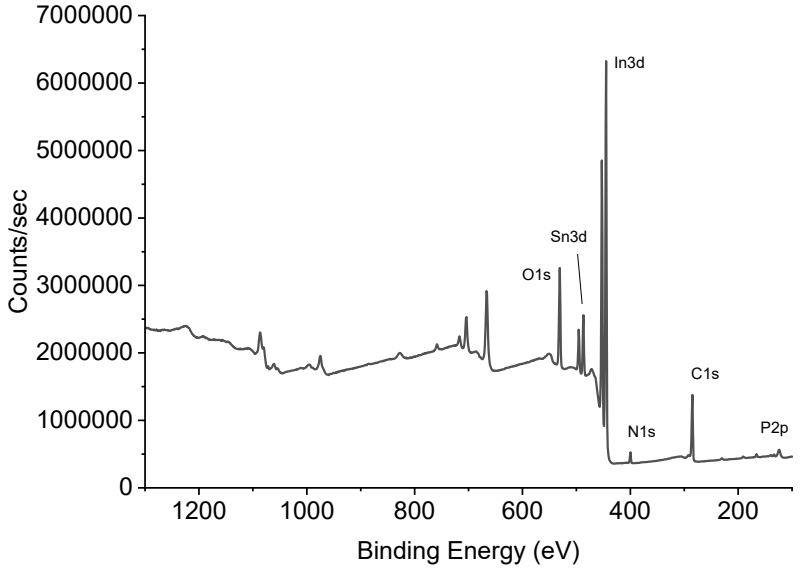

Figure S19. XPS survey spectrum of **1** bound to ITO_{np} showing the different elements present (C, O, P, N) including In and Sn of the substrate .

Table S1. Element ID and their quantitative percentages from the XPS survey spectrum corrected for adventitious carbon.

Atom	BE (eV)	FWHM	Atomic %
In_{3d}	445.6	1.85	8.18
Sn_{3d}	487.1	2.41	1.93
O_{1s}	530.9	2.75	31.10
C_{1s}	285.2	2.29	48.89
N_{1s}	399.9	2.09	4.33
S_{2p}	165.9	2.44	1.54
P_{2p}	133.3	2.33	1.21

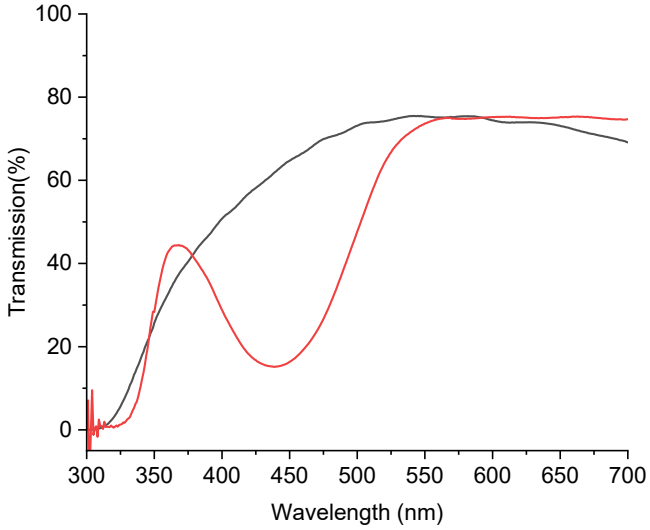

Figure S20. Transmission of ITO_{np} (30% in isopropanol) coated on ITO (black) and **1** bound to ITO_{np} (red).

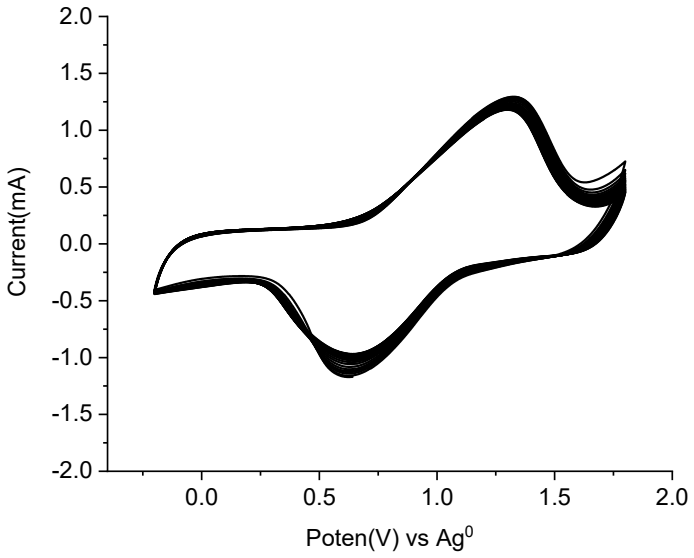

Figure S21. Cyclic voltammogram of **1** bound to ITO_{np} on conductive glass measured in $LiClO_4$ (0.1 M) in propylene carbonate at 50 mV/sec over 10 cycles.

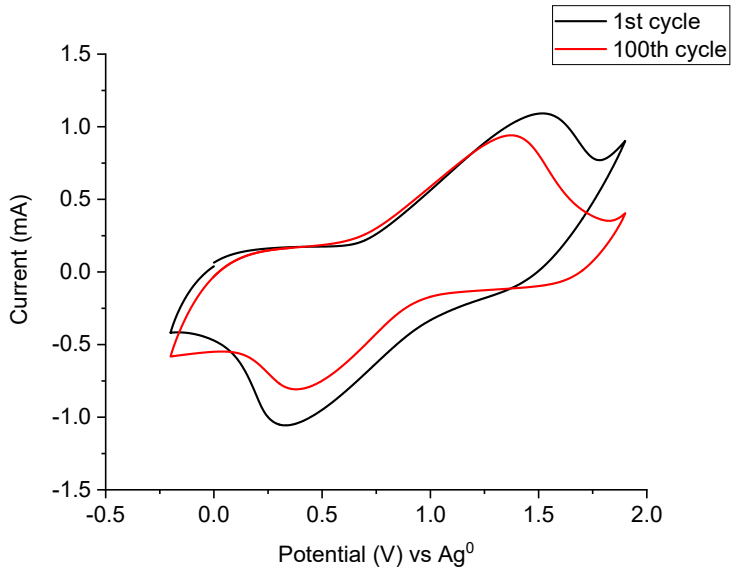

Figure S22. Cyclic voltammogram of **1** bound to ITO_{np} on conductive glass measured in $LiClO_4$ (0.1 M) in propylene carbonate at 50 mV/sec after 100 redox cycles (red) compared to the initial cyclic voltammogram (black).

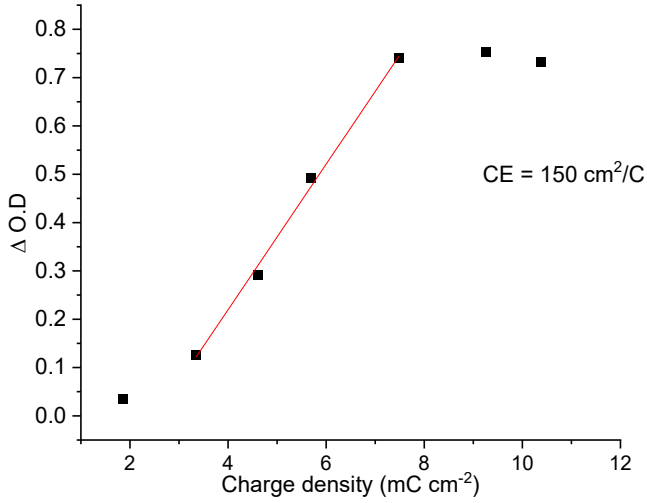

Figure S23. Coloration efficiency determination by change in optical density with charge density.

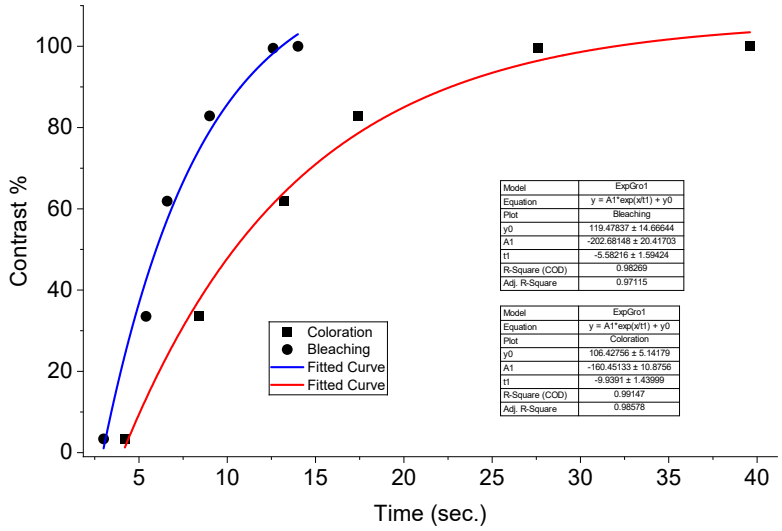

Figure S24. Change in contrast with pulse duration of $\mathbf{1_{np}}$ with 1.2 V for coloration (squares) and bleaching (circles) to determine the universal time constant (τ) by fitting to a first order growth model (line).

Table S2. Comparison of electrochromic performance of molecular electrochromes immobilized via phosphonic acids.

Electrochrome[a]	**ΔT (%) /λ (nm)**[b]	**t_b/t_c (sec)**[c]	**CE**[d]	**Stability**[e]	**EFC**[f]	**Ref.**
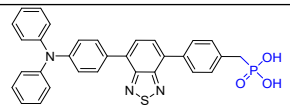	**85 (890)**	**10.2/19.2 (85%)**	**150 cm^2/C (1.095 cm^2; 20 nm film)**	**>120**	**Yes**	**This work**
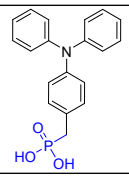	82 (700)	2.6/0.3 (82%)	280 cm^2/C (μM film)	-	No	S3
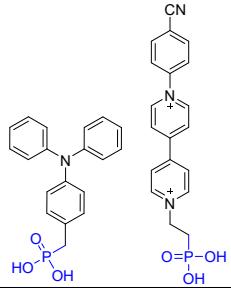	60 (605)	0.6/0.5 (56)	440 cm^2/C (0.095 cm^2; μM film)	-	No	S4
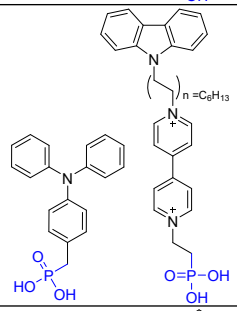	63 (670)	<1 s /1 s (63)	-	>100 000	No	S5
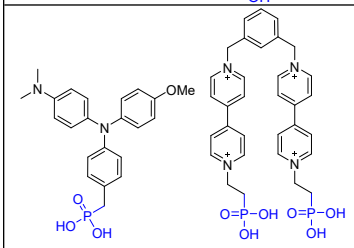	60 (570)	5s/3s (55)	-	>120 000	No	S6

[a] Molecular electrochrome immobilized on substrate via phosphonic acids. [b] Contrast ratio and absorption wavelength monitored for color contrast. [c] Bleaching and coloration kinetics. Values in parentheses correspond to optical transmission percent difference used to measure coloration kinetics. [d] Coloration efficiency. [e] Number of cycles switched between the bleached and colored states. [f] Electrofluorochromism observed.

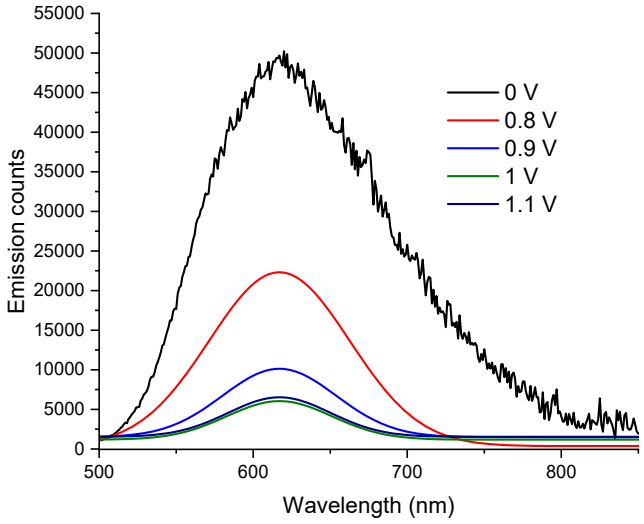

Figure S25. Corrected emission of immobilized **1** on ITO_{np} on conductive glass by removing the residual emission of the electrochemical generated intermediate.

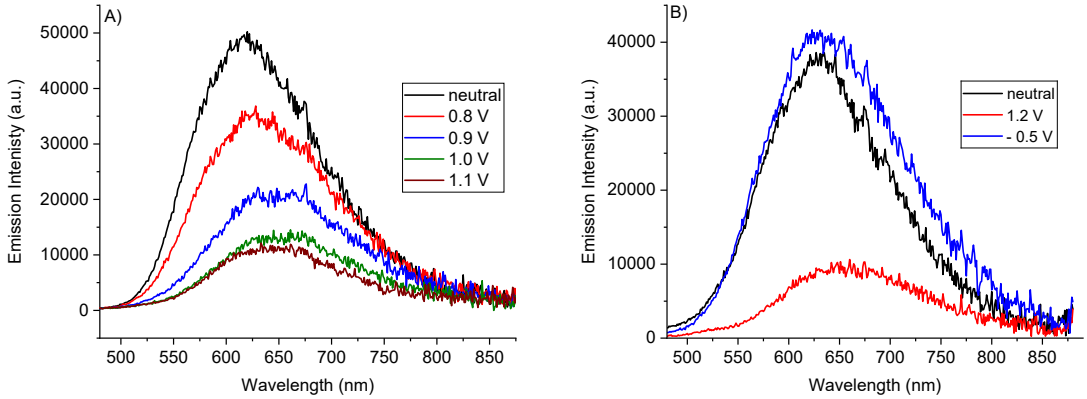

Figure S26 A) Change in fluorescence of **1** coated on ITO_{np} with increasing applied potential excited at 450 nm. B) Change in fluorescence of **1** coated on ITO_{np} switched between its neutral, oxidized, and neutral states, respectively, excited at 450 nm.

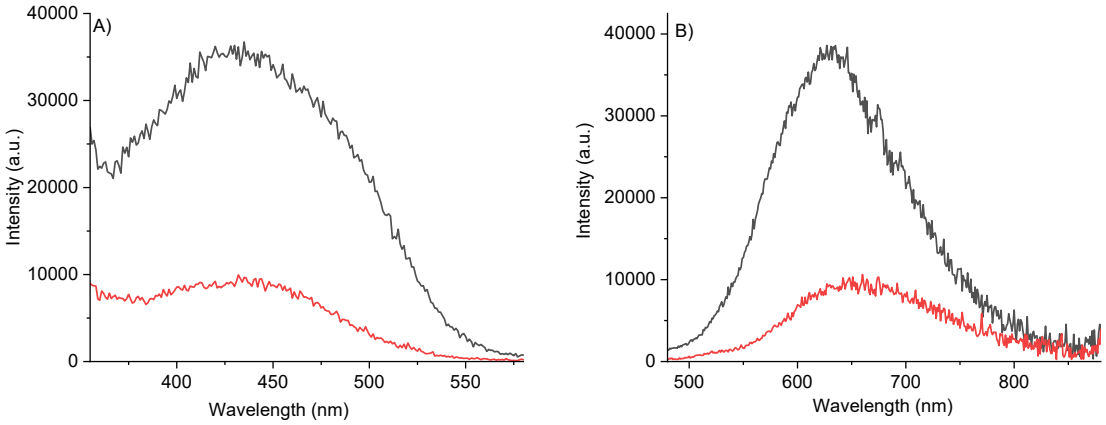

Figure S27 A) Excitation spectra of neutral (black) and oxidized $\mathbf{1}_{np}$ monitoring at 625 nm. B) Emission spectra of neutral (black) and oxidized (red) $\mathbf{1}_{np}$ excited at 450nm.

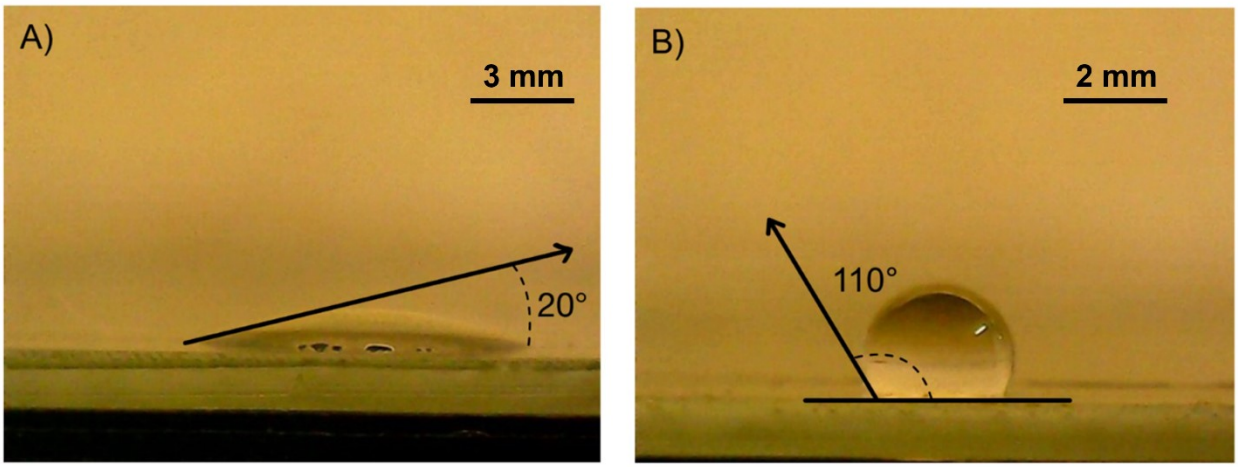

Figure S28. Photographs of a drop of water (water contact) on ITO coated glass before (A) and after (B) impregnation in ethanol solution of **1**.

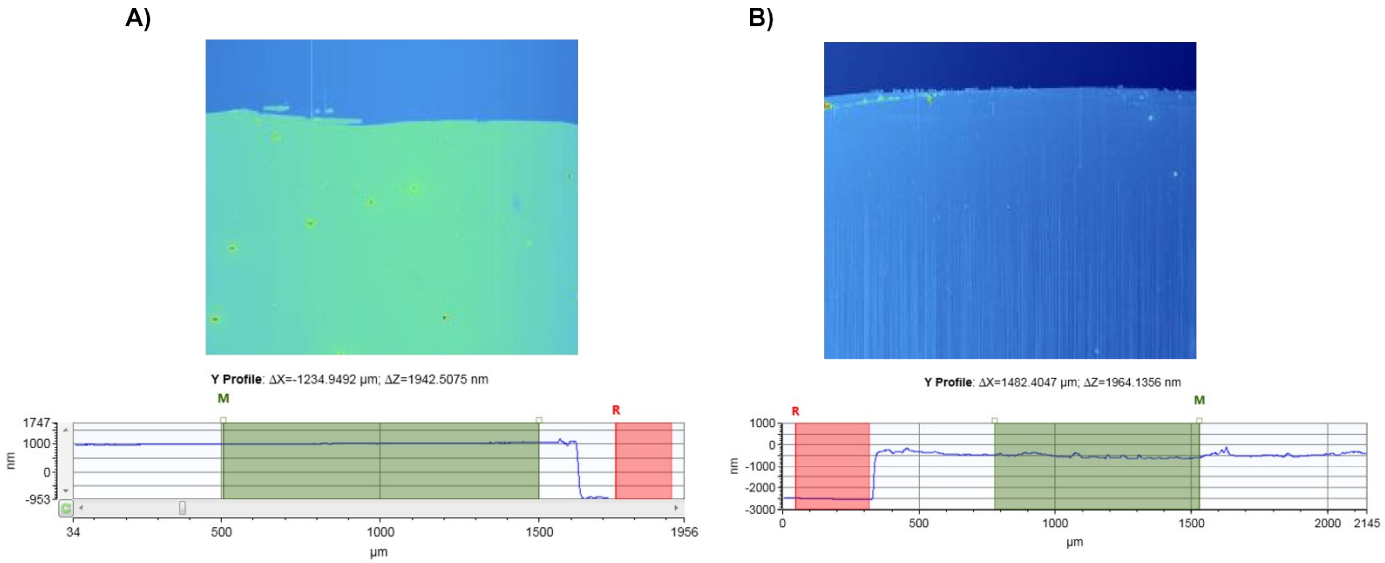

Figure 29. Profiles of the conductive glass coated with ITO_{ns} (A) and coated with **1** (B) measured with a stylus profilometer.

References

S1. Y.-y. Zhu, H.-y. Xia, L.-f. Yao, D.-p. Huang, J.-y. Song, H.-f. He, L. Shen and F. Zhao, *RSC Advances*, 2019, **9**, 7176-7180.

S2. S.-i. Kato, T. Matsumoto, M. Shigeiwa, H. Gorohmaru, S. Maeda, T. Ishi-i and S. Mataka, *Chemistry – A European Journal*, 2006, **12**, 2303-2317.

S3. M. Ciobanu, J. Klein, M. Middendorf, S. M. Beladi Mousavi, F. Carl, M. Haase and L. Walder, *Solar Energy Materials and Solar Cells*, 2019, **203**, 110186.

S4. C. Kortz, A. Hein, M. Ciobanu, L. Walder and E. Oesterschulze, *Nature Communications*, 2019, **10**, 4874.

S5. M. Li, Y. Wei, J. Zheng, D. Zhu and C. Xu, *Organic Electronics*, 2014, **15**, 428-434.

S6. D. Weng, Y. Shi, J. Zheng and C. Xu, *Organic Electronics*, 2016, **34**, 139-145.